

Probing the superconducting ground state of the noncentrosymmetric superconductors CaTSi_3 ($T = \text{Ir, Pt}$) using muon-spin relaxation and rotation

R. P. Singh,¹ A. D. Hillier,² D. Chowdhury,² J. A. T. Barker,¹ D. McK. Paul,¹ M. R. Lees,¹ and G. Balakrishnan¹

¹*Department of Physics, University of Warwick, Coventry, England CV7 7AL, United Kingdom*

²*ISIS, Science and Technology Facilities Council, Rutherford Appleton Laboratory, Harwell Science and Innovation Campus, Oxfordshire, England OX11 0QX, United Kingdom*

(Received 7 May 2014; revised manuscript received 5 August 2014; published 9 September 2014)

The superconducting properties of CaTSi_3 (where $T = \text{Pt}$ and Ir) have been investigated using muon spectroscopy. Our muon-spin-relaxation results suggest that in both these superconductors time-reversal symmetry is preserved, while muon-spin-rotation data show that the temperature dependence of the superfluid density is consistent with an isotropic s -wave gap. The magnetic penetration depths determined from our transverse-field muon-spin-rotation spectra are found to be 448(6) and 150(7) nm for CaPtSi_3 and CaIrSi_3 , respectively.

DOI: [10.1103/PhysRevB.90.104504](https://doi.org/10.1103/PhysRevB.90.104504)

PACS number(s): 74.20.Rp, 74.70.Dd, 76.75.+i

I. INTRODUCTION

There has been a great deal of interest in noncentrosymmetric superconductors (NCSs), instigated by the discovery of the noncentrosymmetric heavy-fermion superconductor CePt_3Si [1]. The absence of a center of inversion in the crystal structure, along with a nontrivial antisymmetric spin-orbit coupling, leads to the intriguing possibility of a superconducting state with an admixture of spin-triplet and spin-singlet pairs. Despite intense theoretical and experimental efforts [2–6] the study of the physics of noncentrosymmetric superconductors remains a dynamic and active field.

One manifestation of unconventional superconductivity is the breaking of time-reversal symmetry (TRS). The magnetic moments associated with the Cooper pairs are nonzero for such superconductors. A local alignment of these moments produces spontaneous, but extremely small, internal magnetic fields. Muon-spin relaxation is especially sensitive to small changes in internal fields and can easily measure fields of ≈ 0.1 G which correspond to moments that are just a few hundredths of a μ_B . Muon-spin relaxation is thus an ideal probe with which to search for TRS breaking [7–10]. Time-reversal symmetry breaking is rare and is only observed directly in a few superconductors, e.g., Sr_2RuO_4 [11], UPt_3 [12], (although not without controversy) [13], $(\text{U,Th})\text{Be}_{13}$ [14], $\text{PrOs}_4\text{Sb}_{12}$ [15], LaNiC_2 [16], $\text{PrPt}_4\text{Ge}_{12}$ [17], $(\text{PrLa})(\text{OsRu})_4\text{Sb}_{12}$ [18], LaNiGa_2 [19], and more recently SrPtAs [20]. The possibility of mixed spin-singlet–spin-triplet pairing in noncentrosymmetric superconductors makes them prime candidates to exhibit TRS breaking [6]. To date, the only truly NCSs reported to show TRS breaking are LaNiC_2 and Re_6Zr [16,21]; however, for LaNiC_2 , a mixing of singlet and triplet states is forbidden due to the symmetry of the structure [22] but is allowed for Re_6Zr .

Many other NCSs have been studied by magnetization, transport, and heat-capacity measurements, e.g., $\text{Nb}_{0.18}\text{Re}_{0.82}$ [23], LaRhSi_3 [24], $\text{Mg}_{10}\text{Ir}_{19}\text{B}_{16}$ [25], $\text{Mo}_3\text{Al}_2\text{C}$ [26], and Re_3W [27], and several have been shown to exhibit unconventional superconducting behavior including features such as upper critical fields close to the Pauli limit, evidence for multiple gaps, or a significant admixture of a triplet component to the superconducting order parameter. Muon spectroscopy studies have been performed on some of these compounds, e.g.,

Re_3W , LaRhSi_3 , LaPtSi_3 , and LaPdSi_3 [24,27,28]. However, no spontaneous fields were observed in the superconducting state in any of these materials. This indicates that TRS breaking is either undetectable or not present in the superconducting state of these compounds.

Muon-spin rotation can be used to accurately determine the magnetic penetration depth λ and hence the temperature dependence of the superfluid density, yielding information on the symmetry of the superconducting gap [7–10]. This technique has been successfully applied to the study of a number of NCSs including Re_3W [27] and LaPtSi_3 [28]. Using muon-spin relaxation and rotation (μSR) together can provide crucial information on the nature and mechanisms of superconductivity in new materials.

Recently a new family of superconducting materials has been discovered with the formula RTX_3 (where $R = \text{rare earth}$, $T = \text{transition metal}$, and $X = \text{Si or Ge}$). These 113 materials can crystallize in either the noncentrosymmetric BaNiSn_3 -type crystal structure (space group $I4mm$) or the centrosymmetric LaRuSn_3 -type cubic structure (space group $Pm\bar{3}n$) shown in Fig. 1. Several 113 materials with a noncentrosymmetric structure such as CeCoSi_3 [29,30], CeRhSi_3 [31,32], and CeIrSi_3 [33,34] exhibit novel ground states. For example, at ambient pressure CeCoSi_3 becomes superconducting at 1.3 K, while CeRhSi_3 and CeIrSi_3 exhibit antiferromagnetic ordering at 1.5 and 5 K, respectively. The latter two compounds also reveal superconductivity under applied pressure. In CeRhSi_3 the superconducting transition temperature T_c increases from 0.45 to 1.1 K between 0.4 and 2.3 GPa [31,32], while for CeIrSi_3 T_c increases from 0.5 to 1.6 K between 1.8 and 2.5 GPa [33]. In these compounds, the competition between the onsite (nonmagnetic) Kondo interaction and the oscillatory intersite long-range magnetic interactions, known as the Rudermann-Kittel-Kasuya-Yosida interaction, plays an important role in the observed and rather unusual physical properties. Replacing Ce with a nonmagnetic analog such as La also produces superconductors which exhibit unusual properties. For example, LaRhSi_3 and LaPdSi_3 are type-I superconductors, whereas LaPtSi_3 is type II [24,28].

In this paper we report on the properties of the new f -electron free 113 compounds, CaIrSi_3 and CaPtSi_3 , both

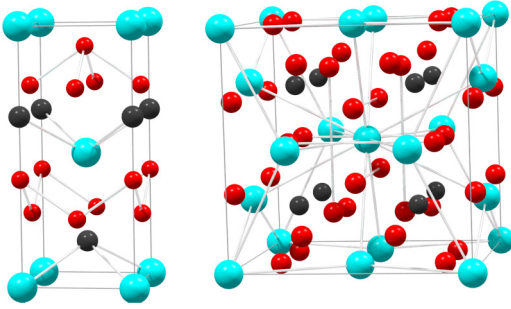


FIG. 1. (Color online) Two possible crystal structures of the RTX_3 (113) compounds. Left is the noncentrosymmetric structure with the space group $I4mm$ and right is the centrosymmetric structure with the space group $Pm\bar{3}n$. The light (blue) spheres are the R atoms, the black spheres are the T atoms, and the dark (red) spheres are the X atoms.

of which have the potential to be of great interest. CaIrSi_3 and CaPtSi_3 are NCSs with superconducting transition temperatures of 3.6 and 2.3 K, respectively, and therefore do not require pressure to induce the superconducting state unlike their Ce analogs [35,36]. Specific-heat data are in general agreement with these superconductors being fully gapped; however, CaIrSi_3 appears to show a deviation from a pure s -wave gap, which has been suggested as evidence for a multiband or anisotropic gap [35]. In the presence of Ir and Pt it is expected that spin-orbit coupling will be significant, strengthening the possibility that the mechanisms for superconductivity might not be entirely conventional in these materials. Therefore, it is timely and interesting to probe the superconducting state of CaIrSi_3 and CaPtSi_3 using muon spectroscopy. In this work, muon-spin relaxation is used to search for evidence of TRS breaking in these two superconductors. Muon-spin rotation is used to determine the temperature-dependent magnetic penetration depth. Since $\lambda(T)$ is directly related to the superfluid density, the pairing symmetry can then be determined.

II. EXPERIMENTAL DETAILS

A. Sample preparation

Polycrystalline samples of CaPtSi_3 and CaIrSi_3 were prepared by arc melting stoichiometric quantities of high-purity Ca (5% excess of Ca to compensate for any weight loss), Pt/Ir, and Si in a tri-arc furnace under an argon (5N) atmosphere on a water-cooled copper hearth. In order to minimize the loss of the Ca by evaporation, melting is done in two steps. In the first step, Pt/Ir are melted with Si. The observed weight loss during the melting of binaries Pt/Ir-Si is negligible. In the second step, Pt/Ir-Si binaries are melted with 5% excess of Ca. The sample buttons were melted and flipped several times to improve phase homogeneity.

B. Sample characterization

Powder x-ray-diffraction data were collected for both samples. Refinement of the x-ray data (see Table I) confirmed that both the samples had the tetragonal structure [space group $I4mm$ (No. 107)] with lattice parameters which are in good

TABLE I. Lattice parameters of noncentrosymmetric CaPtSi_3 and CaIrSi_3 determined from powder x-ray-diffraction data collected at 298 K.

	CaPtSi_3	CaIrSi_3
Structure	Tetragonal	Tetragonal
Space group	$I4mm$	$I4mm$
a (nm)	0.42182(5)	0.41957(2)
c (nm)	0.9880(2)	0.98711(7)

agreement with those reported earlier [35]. There are some impurity peaks present in both the CaIrSi_3 and CaPtSi_3 samples at the same positions observed by Eguchi *et al.* [35].

In order to confirm the superconducting transition temperatures of the samples, dc magnetic susceptibility measurements were made using a Quantum Design magnetic property measurement system. Figure 2 shows the magnetic susceptibility as a function of temperature in an applied field of 5 Oe. The observed superconducting transition temperatures T_C for CaPtSi_3 and CaIrSi_3 are approximately 2.3 and 3.5 K, respectively (see Table II). These transition temperatures are in good agreement with previously reported results measured by dc susceptibility on samples with the same composition

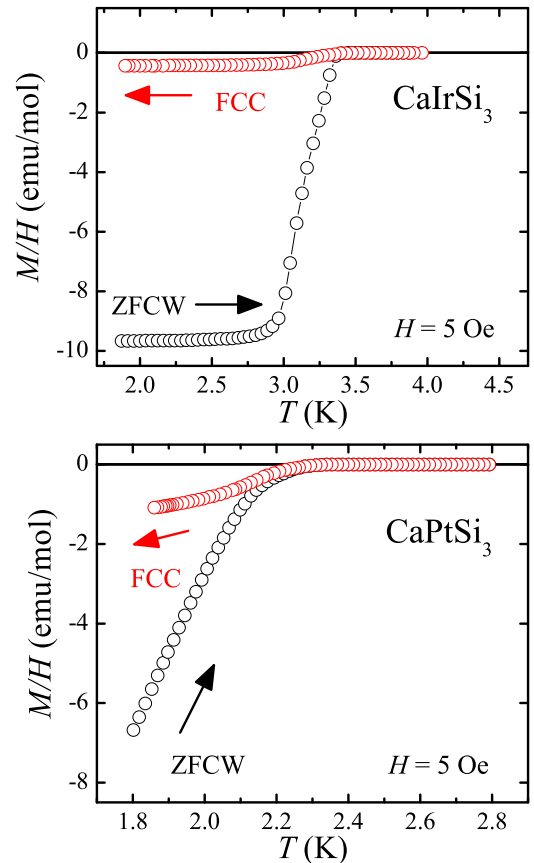


FIG. 2. (Color online) Temperature dependence of the dc magnetization for CaIrSi_3 (upper) and CaPtSi_3 (lower). The samples were cooled in zero field and a field of 5 Oe was then applied. Data were collected on zero-field-cooled warming (ZFCW) and during a subsequent field-cooled cooling (FCC) in the same applied field.

TABLE II. Superconducting parameters of noncentrosymmetric CaPtSi_3 and CaIrSi_3 determined from the dc magnetization and muon spectroscopy data.

	CaPtSi_3	CaIrSi_3
T_c (K)	2.30(5)	3.50(5)
$\lambda(0)$ (nm)	448(6)	150(7)
$\Delta(0)$ (meV)	0.38(1)	0.81(1)
BCS ratio	3.8(2)	5.4(2)

[35]. There is no evidence from the dc susceptibility data that the impurities present in our samples order magnetically or become superconducting. Since muon spectroscopy probes the full volume of the sample the results presented below are representative of the majority of superconducting phases.

C. Muon spectroscopy

The muon-spin-relaxation measurements in zero field (ZF) and muon-spin-rotation experiments in transverse fields (TFs), were carried out at the ISIS pulsed neutron and muon facility using the MuSR spectrometer [37]. At the ISIS facility, a pulse of protons with a full width at half maximum of ≈ 70 ns are produced every 20 ms, with four out of five pulses going through the muon target. The muons produced are implanted into the sample and decay with an average lifetime of 2.2 μs into a positron which is emitted preferentially in the direction of the muon-spin axis along with two neutrinos. These positrons are detected and time stamped in the 64 detectors which are positioned either before, F , or after, B , the sample for longitudinal (relaxation) experiments. The asymmetry A of the μSR time spectrum is then obtained as $A(t) = [F(t) - \alpha B(t)]/[F(t) + \alpha B(t)]$, where α represents a relative counting efficiency of the forward and backward detectors [8,10]. Using these counts the asymmetry in the positron emission can be determined and, therefore, the muon polarization is measured as a function of time.

For the transverse-field experiments, a magnetic field is applied perpendicular to the initial muon-spin direction and momentum. In this configuration, the signals from the instrument's 64 detectors are normalized and reduced to two orthogonal components which are then fitted simultaneously.

Powder samples of each material were mixed with GE varnish and mounted onto silver holders. Any muons which stop in silver give a time-independent background for ZF- μSR experiments and a nondecaying precession signal in the TF μSR . The sample holder and sample were mounted into a helium-3 cryostat with a temperature range of 0.3 to 50 K. The samples were cooled to base temperature in zero field and the relaxation spectra were collected at fixed temperature upon warming while still in zero field. The stray fields at the sample position were canceled to within 10 mG by a flux-gate magnetometer and an active compensation system controlling three pairs of correction coils. The TF- μSR experiments were conducted in a range of applied fields from 50 to 600 Oe. The field was applied above the superconducting transition before cooling.

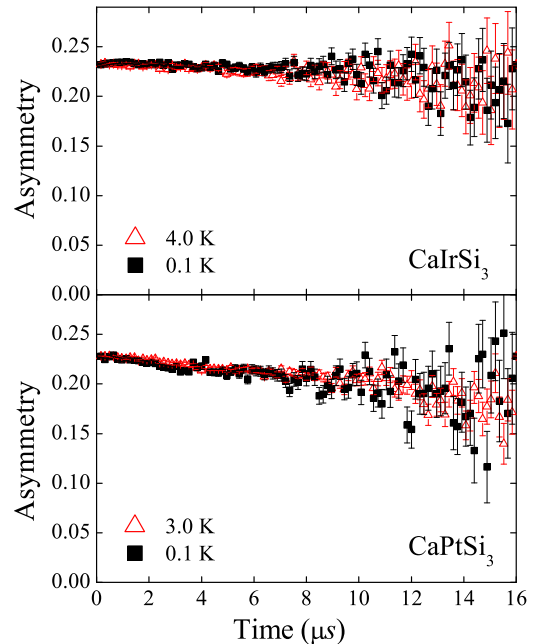


FIG. 3. (Color online) Zero-field muon-spin-relaxation spectra for CaIrSi_3 (upper panel) and CaPtSi_3 (lower panel) at temperatures above (open symbols) and below (closed symbols) T_c .

III. RESULTS AND DISCUSSION

A. Zero-field muon-spin relaxation

First, let us consider the zero-field muon-spin-relaxation results (see Fig. 3). The absence of an oscillation in the ZF- μSR asymmetry data at all temperatures for both samples confirms that there are no coherent magnetic fields, usually, associated with long-range magnetic order. In the absence of atomic moments, in CaTSi_3 the muon-spin relaxation is expected to arise from the local fields associated with nuclear moments. These moments are usually static on the time scale of the muon and are randomly orientated. In a case such as this the depolarization function can be described by a Kubo-Toyabe function [8,10]. In Fig. 3, we can see that for both CaIrSi_3 and CaPtSi_3 the data are relatively flat and do not have the characteristic shape of the aforementioned Kubo-Toyabe function. This indicates that the fields from the nuclear moments are small. Moreover, the μSR signals for temperatures above and below the superconducting transition overlay and the depolarization rate are the same. This indicates that time-reversal symmetry is preserved, as would be expected in a conventional singlet superconductor, or at least that any symmetry-breaking field is not observable by μSR .

B. Transverse-field muon-spin rotation

Transverse-field muon-spin rotation can be used to determine the magnetic penetration depth λ . Figure 4 shows typical spectra with a transverse applied field of 100 Oe at $T = 0.2, 1.1,$ and 1.95 K after being cooled through T_c . The TF- μSR spectra were fit as a sum of sinusoidally oscillating

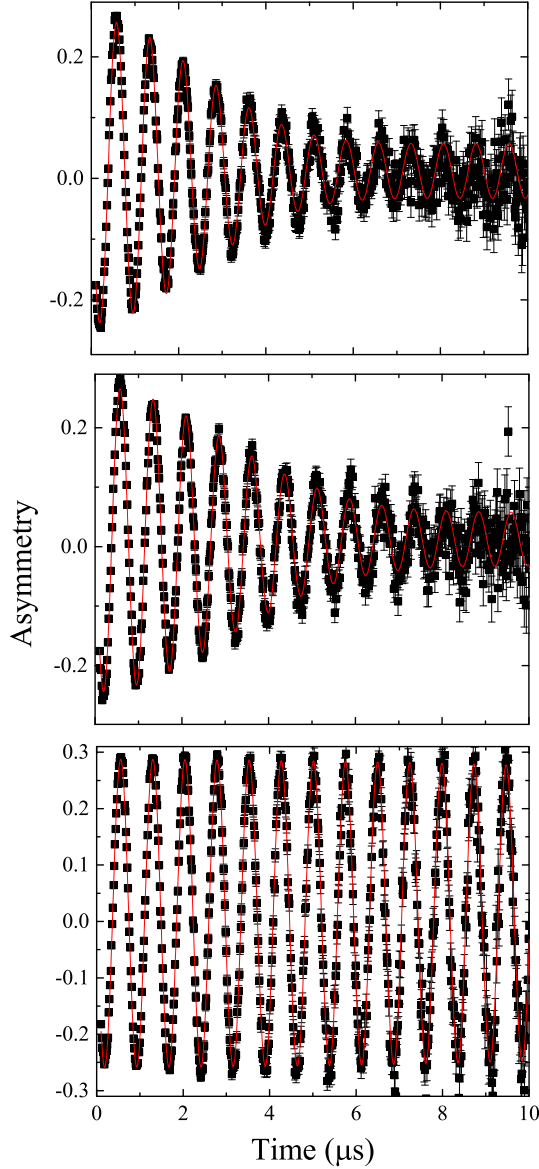


FIG. 4. (Color online) Typical muon-spin-rotation spectra for CaPtSi₃ in a transverse field of 100 Oe at temperatures of 0.2 K (upper), 1.1 K (middle), and 1.95 K (lower). The lines are fits to the data using Eq. (1) as described in the text.

components, each within a Gaussian relaxation envelope:

$$G_x(t) = \sum_{i=1}^n A_i \exp\left(-\frac{\sigma_i^2 t^2}{2}\right) \cos(\gamma_\mu B_i t + \varphi), \quad (1)$$

where A_i is the initial asymmetry, σ_i is the Gaussian relaxation rate, and B_i is the first moment for the i th component of the field distribution [38,39]. There is a common phase offset φ , and γ_μ is the muon gyromagnetic ratio. In these fits, σ_n for the n th component is set to zero and corresponds to a background term arising from those muons which are implanted into the silver sample holder producing an oscillating signal that has no depolarization, as silver has a negligible nuclear moment. Using Eq. (1) is equivalent to assuming a field distribution

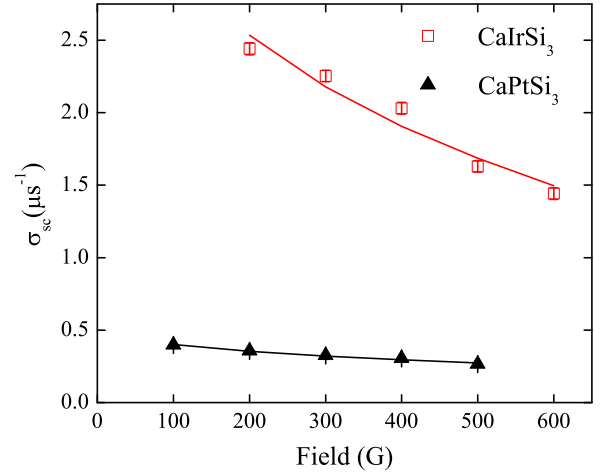


FIG. 5. (Color online) Field dependence of the muon depolarization rate at $T = 100$ mK for CaIrSi₃ (open symbols) and CaPtSi₃ (closed symbols). The lines are fits to the data using Eq. (4) as described in the text.

$P(B)$ within the sample given by

$$P(B) = \gamma_\mu \sum_{i=1}^{n-1} \frac{A_i}{\sigma_i} \exp\left(-\frac{\gamma_\mu^2 (B - B_i)^2}{2\sigma_i^2}\right). \quad (2)$$

The second moment of the field distribution within the sample $\langle \Delta B^2 \rangle$ is

$$\langle \Delta B^2 \rangle = \left(\frac{\sigma}{\gamma_\mu}\right)^2 = \sum_{i=1}^{n-1} \frac{A_i}{A_{\text{tot}}} \left[\left(\frac{\sigma_i}{\gamma_\mu}\right)^2 + (B_i - \langle B \rangle)^2 \right], \quad (3)$$

where $A_{\text{tot}} = \sum_{i=1}^{n-1} A_i$ and $\langle B \rangle = \sum_{i=1}^{n-1} \frac{A_i B_i}{A_{\text{tot}}}$. The superconducting component of the second moment σ_{SC} is then given by $\sigma_{\text{SC}}^2 = \sigma^2 - \sigma_{\text{nm}}^2$ where σ_{nm}^2 is the signal in the normal state due to the nuclear moments.

The spectra from the CaIrSi₃ were best described by three oscillating functions whereas the spectra from the CaPtSi₃ could be described by just two [38]. The field dependences of the superconducting depolarization rates σ_{SC} are shown in Fig. 5. As the field increases the depolarization rates decrease as may be expected for a superconductor when the applied field is a significant fraction of the upper critical field B_{c2} [9]. The field dependence of σ_{SC} can be used to determine the magnetic penetration depth and to give an estimate for the upper critical field (see Fig. 5). B_{c2} can be independently verified using other measurements. The $\sigma_{\text{SC}}(B)$ data shown in Fig. 5 were fit using Eq. (4):

$$\sigma_{\text{SC}}[\mu\text{s}^{-1}] = A \times (1 - b)[1 + 1.21(1 - \sqrt{b})^3] \lambda^{-2}(\text{in nm}), \quad (4)$$

where λ is in nm, $b = B/B_{c2}$ is the ratio of the applied field to the upper critical field, and A is a prefactor related to the structure of the flux-line lattice ($A = 4.83 \times 10^4$ for a hexagonal lattice) [40,41]. Assuming the penetration depth either follows a two-fluid model $\{\lambda^{-2}(T)/\lambda^{-2}(0) = [1 - (T/T_c)^4]\}$ or can be described using the local (London) approximation for an s -wave gap superconductor (see below) gives penetration depths $\lambda(0)$ of 448(6) and 150(7) nm for CaPtSi₃ and CaIrSi₃,

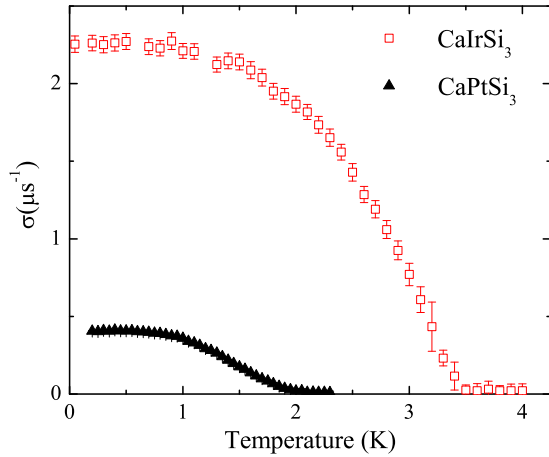


FIG. 6. (Color online) Temperature dependence of the muon depolarization rate σ for CaPtSi₃ (closed symbols) and CaIrSi₃ (open symbols).

respectively. The upper critical fields estimated from the σ_{SC} versus B data and from extrapolations to 0 K of the $B_{c2}(T)$ curves determined from $M(H)$ loops collected at temperatures above 1.5 K (data not shown) are in good agreement with those reported by Eguchi *et al.* [35] from magnetic and transport data, although as in Ref. [35] there is considerable uncertainty associated with these estimates. More comprehensive data sets down to low temperatures are required to accurately determine $B_{c2}(0)$ for both materials.

The temperature dependences of the muon depolarization rate σ for CaPtSi₃ and CaIrSi₃ are given in Fig. 6. For both samples, the data show a plateau and then decrease as the temperature is increased. σ then levels off at a temperature slightly less than T_c . The depolarization rates at higher temperatures ($T \geq T_c$) are small, in agreement with the zero-field data discussed above. This depolarization σ_{nm} is associated with the nuclear moments. Below T_c , the depolarization rates are related to the magnetic penetration depth [see Eq. (4)] and therefore the structure of the superconducting gaps for the two materials can be investigated. After subtracting σ_{nm} from σ to give σ_{SC} as described above, λ can be calculated at each temperature, with a correction for the strong-field dependence of the depolarization rates made using the $B_{c2}(T)$ data from [35] and Eq. (4). The temperature dependences of $\lambda(T)$ determined in this way for CaPtSi₃ and CaIrSi₃ and plotted as $\lambda^{-2}(T)/\lambda^{-2}(0)$ versus the reduced temperature T/T_c are shown in Fig. 7. The $\lambda(T)$ curves can then be fit within the local (London) approximation [42] for an s -wave gap superconductor in the clean limit using the following expression:

$$\frac{\lambda^{-2}(T)}{\lambda^{-2}(0)} = 1 + 2 \int_{\Delta(T)}^{\infty} \left(\frac{\partial f}{\partial E} \right) \frac{E}{\sqrt{E^2 - \Delta^2(T)}} dE, \quad (5)$$

where $f = [1 + \exp(E/k_B T)]^{-1}$ is the Fermi function. The temperature dependence of the gap is approximated by $\Delta(T) = \Delta(0) \tanh\{1.82[1.018(T_c/T - 1)]^{0.51}\}$ [43]. As can be seen from Fig. 7 the temperature dependence of σ_{SC} for both samples is very well described by this isotropic s -wave model giving $\Delta(0) = 0.81(1)$ and $0.38(1)$ meV and BCS ratios

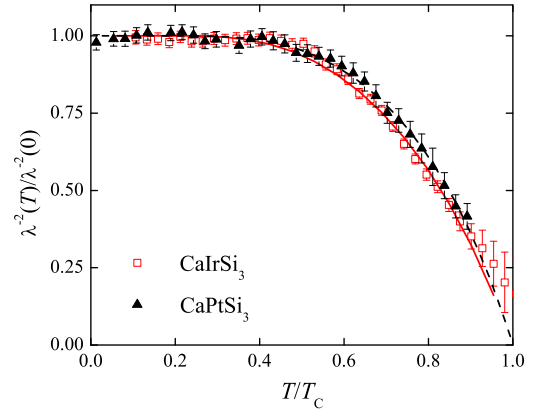


FIG. 7. (Color online) Normalized inverse square of the London penetration depth (the superfluid density) $\lambda^{-2}(T)/\lambda^{-2}(0)$ vs the reduced temperature T/T_c for CaPtSi₃ and CaIrSi₃. The lines are fits to the data as described in the text. The closed symbols and solid line are the data and fit for the CaPtSi₃, and the open symbols and dashed line are the data and fit for CaIrSi₃.

$2\Delta(0)/k_B T_c$ of 3.8(2) and 5.4(2) for CaPtSi₃ and CaIrSi₃, respectively. The value of the BCS ratio for CaPtSi₃ is slightly higher than the 3.5 expected in the weak-coupling limit. The higher value obtained for CaIrSi₃, along with the strong-field dependence of σ_{SC} shown in Fig. 5, could be evidence of a strong-coupling and/or multigap behavior with each gap having a similar temperature dependence. Such a suggestion is consistent with the departure from a pure s -wave behavior seen in the specific heat of CaIrSi₃, although the specific-heat results for CaIrSi₃ are generally well explained by a weak-coupling BCS theory [35].

IV. SUMMARY

In summary, we have investigated the superconducting compounds CaPtSi₃ and CaIrSi₃ by using muon-spin relaxation and rotation. There is no evidence of time-reversal symmetry breaking in either material, at least within the sensitivity of μ SR. The superconducting parameters determined from this study are summarized in Table II. The temperature dependences of the penetration depths for both materials are consistent with s -wave isotropic gaps. The BCS ratios place both materials in the intermediate- to strong-coupling limit.

ACKNOWLEDGMENTS

We acknowledge the Engineering and Physical Sciences Research Council, UK, for providing funding (Grant No. EP/I007210/1). We thank T. E. Orton for technical support. Some of the equipment used in this research at the University of Warwick was obtained through the Science City Advanced Materials: Creating and Characterizing Next Generation Advanced Materials Project, with support from Advantage West Midlands and partly funded by the European Regional Development Fund.

- [1] E. Bauer, G. Hilscher, H. Michor, Ch. Paul, E. W. Scheidt, A. Griбанov, Yu. Seropugin, H. Noël, M. Sigrist, and P. Rogl, *Phys. Rev. Lett.* **92**, 027003 (2004).
- [2] L. P. Gor'kov and E. I. Rashba, *Phys. Rev. Lett.* **87**, 037004 (2001).
- [3] P. A. Frigeri, D. F. Agterberg, A. Koga, and M. Sigrist, *Phys. Rev. Lett.* **92**, 097001 (2004).
- [4] P. A. Frigeri, D. F. Agterberg, I. Milat, and M. Sigrist, *Eur. Phys. J. B* **54**, 435 (2006).
- [5] M. Sigrist, *AIP Conf. Proc.* **1162**, 55 (2009).
- [6] E. Bauer and M. Sigrist, *Non-Centrosymmetric Superconductors: Introduction and Overview*, Lecture Notes in Physics Vol. 847 (Springer-Verlag, Berlin, 2012).
- [7] A. Schenck, *Muon Spin Rotation Spectroscopy Principles and Applications in Solid State Physics* (Taylor & Francis, London, 1985).
- [8] S. L. Lee, S. H. Kilcoyne, and R. Cywinski, *Muon Science: Muons in Physics, Chemistry and Materials* (Taylor & Francis, London, 1999).
- [9] J. E. Sonier, *Rep. Prog. Phys.* **70**, 1717 (2007).
- [10] A. Yaouanc and P. D. de Réotier, *Muon Spin Rotation, Relaxation, and Resonance* (Oxford University Press, Oxford, 2011).
- [11] G. M. Luke, Y. Fudamoto, K. M. Kojima, M. I. Larkin, J. Merrin, B. Nachumi, Y. J. Uemura, Y. Maeno, Z. Q. Mao, Y. Mori *et al.*, *Nature (London)* **394**, 558 (1998).
- [12] G. M. Luke, A. Keren, L. P. Le, W. D. Wu, Y. J. Uemura, D. A. Bonn, L. Taillefer, and J. D. Garrett, *Phys. Rev. Lett.* **71**, 1466 (1993).
- [13] P. D. de Réotier, A. Huxley, A. Yaouanc, J. Flouquet, P. Bonville, P. Impert, P. Pari, P. C. M. Gubbens, and A. M. Mulders, *Phys. Lett. A* **205**, 239 (1995).
- [14] R. H. Heffner, J. L. Smith, J. O. Willis, P. Birrer, C. Baines, F. N. Gyax, B. Hitti, E. Lippelt, H. R. Ott, A. Schenck *et al.*, *Phys. Rev. Lett.* **65**, 2816 (1990).
- [15] Y. Aoki, A. Tsuchiya, T. Kanayama, S. R. Saha, H. Sugawara, H. Sato, W. Higemoto, A. Koda, K. Ohishi, K. Nishiyama *et al.*, *Phys. Rev. Lett.* **91**, 067003 (2003).
- [16] A. D. Hillier, J. Quintanilla, and R. Cywinski, *Phys. Rev. Lett.* **102**, 117007 (2009).
- [17] A. Maisuradze, W. Schnelle, R. Khasanov, R. Gumeniuk, M. Nicklas, H. Rosner, A. Leithe-Jasper, Yu. Grin, A. Amato, and P. Thalmeier, *Phys. Rev. B* **82**, 024524 (2010).
- [18] L. Shu, W. Higemoto, Y. Aoki, A. D. Hillier, K. Ohishi, K. Ishida, R. Kadono, A. Koda, O. O. Bernal, D. E. MacLaughlin *et al.*, *Phys. Rev. B* **83**, 100504 (2011).
- [19] A. D. Hillier, J. Quintanilla, B. Mazidian, J. F. Annett, and R. Cywinski, *Phys. Rev. Lett.* **109**, 097001 (2012).
- [20] P. K. Biswas, H. Luetkens, T. Neupert, T. Stürzer, C. Baines, G. Pascua, A. P. Schnyder, M. H. Fischer, J. Goryo, M. R. Lees *et al.*, *Phys. Rev. B* **87**, 180503 (2013).
- [21] R. P. Singh, A. D. Hillier, B. Mazidian, J. Quintanilla, J. F. Annett, D. McK. Paul, G. Balakrishnan, and M. R. Lees, *Phys. Rev. Lett.* **112**, 107002 (2014).
- [22] J. Quintanilla, A. D. Hillier, J. F. Annett, and R. Cywinski, *Phys. Rev. B* **82**, 174511 (2010).
- [23] A. B. Karki, Y. M. Xiong, I. Vekhter, D. Browne, P. W. Adams, D. P. Young, K. R. Thomas, J. Y. Chan, H. Kim, and R. Prozorov, *Phys. Rev. B* **82**, 064512 (2010).
- [24] V. K. Anand, A. D. Hillier, D. T. Adroja, A. M. Strydom, H. Michor, K. A. McEwen, and B. D. Rainford, *Phys. Rev. B* **83**, 064522 (2011).
- [25] T. Klimczuk, F. Ronning, V. Sidorov, R. J. Cava, and J. D. Thompson, *Phys. Rev. Lett.* **99**, 257004 (2007).
- [26] A. B. Karki, Y. M. Xiong, N. Haldolaarachchige, S. Stadler, I. Vekhter, P. W. Adams, D. P. Young, W. A. Phelan, and J. Y. Chan, *Phys. Rev. B* **83**, 144525 (2011).
- [27] P. K. Biswas, M. R. Lees, A. D. Hillier, R. I. Smith, W. G. Marshall, and D. M. Paul, *Phys. Rev. B* **84**, 184529 (2011).
- [28] M. Smidman, A. D. Hillier, D. T. Adroja, M. R. Lees, V. K. Anand, R. P. Singh, R. I. Smith, D. M. Paul, and G. Balakrishnan, *Phys. Rev. B* **89**, 094509 (2014).
- [29] P. Haen, P. Lejay, B. Chevalier, B. Lloret, J. Etourneau, and M. Sera, *J. Less-Common Met.* **110**, 321 (1985).
- [30] Y. Iwamoto, K. Ueda, T. Kohara, and Y. Yamada, *Physica B* **206-207**, 276 (1995).
- [31] N. Kimura, K. Ito, K. Saitoh, Y. Umeda, H. Aoki, and T. Terashima, *Phys. Rev. Lett.* **95**, 247004 (2005).
- [32] N. Kimura, K. Ito, H. Aoki, S. Uji, and T. Terashima, *Phys. Rev. Lett.* **98**, 197001 (2007).
- [33] I. Sugitani, Y. Okuda, H. Shishido, T. Yamada, A. Thamizhavel, E. Yamamoto, T. D. Matsuda, Y. Haga, T. Takeuchi, R. Settai *et al.*, *J. Phys. Soc. Jpn.* **75**, 043703 (2006).
- [34] H. Mukuda, T. Fujii, T. Ohara, A. Harada, M. Yashima, Y. Kitaoka, Y. Okuda, R. Settai, and Y. Onuki, *Phys. Rev. Lett.* **100**, 107003 (2008).
- [35] G. Eguchi, D. C. Peets, M. Kriener, Y. Maeno, E. Nishibori, Y. Kumazawa, K. Banno, S. Maki, and H. Sawa, *Phys. Rev. B* **83**, 024512 (2011).
- [36] G. Eguchi, D. Peets, M. Kriener, S. Maki, E. Nishibori, H. Sawa, and Y. Maeno, *Physica C* **470**, S762 (2010).
- [37] P. J. C. King, R. de Renzi, S. P. Cottrell, A. D. Hillier, and S. F. J. Cox, *Phys. Scripta* **88**, 068502 (2013).
- [38] A. Maisuradze, R. Khasanov, A. Shengelaya, and H. Keller, *J. Phys.: Condens. Matter* **21**, 075701 (2009).
- [39] M. Weber, A. Amato, F. N. Gyax, A. Schenck, H. Maletta, V. N. Duginov, V. G. Grebinnik, A. B. Lazarev, V. G. Olshevsky, V. Y. Pomjakushin *et al.*, *Phys. Rev. B* **48**, 13022 (1993).
- [40] E. H. Brandt, *J. Low Temp. Phys.* **73**, 355 (1988).
- [41] E. H. Brandt, *Phys. Rev. B* **68**, 054506 (2003).
- [42] M. Tinkham, *Introduction to Superconductivity*, 2nd ed. (McGraw-Hill, New York, 1996).
- [43] A. Carrington and F. Manzano, *Physica C* **385**, 205 (2003).